

Received March 27, 2020, accepted April 11, 2020, date of publication April 17, 2020, date of current version May 1, 2020.

Digital Object Identifier 10.1109/ACCESS.2020.2988552

# Multichannel Signal Denoising Using Multivariate Variational Mode Decomposition With Subspace Projection

PEIPEI CAO<sup>1,3</sup>, HUALI WANG<sup>2</sup>, (Member, IEEE), AND KAIJIE ZHOU<sup>2,3</sup>

<sup>1</sup>School of Electronic and Optical Engineering, Nanjing University of Science and Technology, Nanjing 210094, China

<sup>2</sup>Institute of Communications Engineering, Army Engineering University, Nanjing 210007, China

<sup>3</sup>College of Physics and Electrical Engineering, Huaiyin Normal University, Huai'an 223300, China

Corresponding author: Huali Wang (huali.wang@ieee.org)

**ABSTRACT** This paper describes a novel multichannel signal denoising approach based on multivariate variational mode decomposition (MVMD). MVMD is the extended version of the variational mode decomposition (VMD) algorithm for multichannel data sets. Unlike previous MEMD (multivariate empirical mode decomposition)-based denoising methods, the proposed scheme not only has a precise mathematical framework but also can better align the common frequency modes of the signals. Therefore, it has good robustness for non-stationary signals with low SNR. Based on the similarity measurement between the probability density function (pdf) of the input signal and each mode by Hausdorff distance (HD), the interval thresholding and partial reconstruction denoising of band-limited intrinsic mode functions (BLIMFs) are performed in the algorithm. Besides, to take advantage of the characteristics of channel diversity, the subspace projection method is used to further denoise the multivariable signals. We demonstrate the effectiveness of the proposed approach through results obtained from extensive simulations involving test (synthetic) and real-world multivariate data set.

**INDEX TERMS** MVMD, VMD, oscillatory modes.


## I. INTRODUCTION

Removing white gaussian noise (WGN) from interested data is very important in real signal processing applications. For example, in communication and network applications, noise from data acquisition equipment (sensors), thermal noise from atomic vibration in conductors, and quantization noise can be effectively modeled by independent Gaussian distribution.

In recent years, the development of data acquisition tools has emphasized the need to process multi-channel (multivariate) data directly, from communication [1] to biomedicine [2]. To realize joint denoising of multi-channel signals, a multivariate extension of single-variable wavelet denoising (MWD) was proposed in [3]. This method combined  $N$  univariate wavelet denoising with principal component analysis (PCA) of the observed signal, which has a better denoising effect than the traditional channel-based wavelet denoising

method. In addition, a similar multivariate wavelet denoising method is proposed in [4]. Both of them are sensitive to channel offset. Lately, synchrosqueezing transform (SST) has been used in multivariable denoising (MWSD), which takes into account the threshold technology of the multivariable oscillation [5]. When the signal has a fixed frequency in the analysis window, this algorithm is proved to be very effective for multivariable denoising. However, in most cases, the received signal shows a large frequency hopping. In this case, the performance of the denoising method based on SST deteriorates. Furthermore, the calculation of synchrosqueezing transform based on wavelet is also time-consuming, which is not fit for real-time signal processing.

EMD which is now widely used to recursively decompose signals into different modes of unknown but independent spectral bands. Empirical mode decomposition is a completely adaptive data-driven tool for non-stationary signal decomposition [6]. Multivariate empirical mode decomposition based interval thresholding method (MEMD-IT) was proposed in [7], IMFs were selected for partial reconstruction

The associate editor coordinating the review of this manuscript and approving it for publication was Wei Liu .

by using mode alignment characteristics. However, the interval threshold is used on the channel and does not take into account the correlation in the same index IMFs. Hence, [8] mainly introduces a subspace denoising method based on multivariate extensions of empirical mode decomposition (MEMD), here we call this method MEMD-SP. But mode-mixing among different channels of MEMD [9] is also problematic. In 2017, MEMD-ITSP method was used to denoise the multivariable signals and further to utilize the channel diversity in [10]. Due to the lack of mathematical theory and specified degrees of freedom, the robustness of the algorithm is reduced.

To overcome this problem, Dragomiretskiy and Zosso [11] proposed a non-recursive algorithm, the variational mode decomposition (VMD) model, which is similar to the EMD algorithm. Compared to EMD, VMD can adaptively decompose any signal into a set of band-limited intrinsic mode functions (BLIMFs), estimate its center frequency online, and extract all modes simultaneously. Therefore, VMD is suitable for removing noise in non-stationary signals. In 2017, [12] proposed variational mode decomposition denoising combined with the Hausdorff distance, the filtering results obtained by this method showed the better effectiveness of this method compared with EMD-based method. Li *et al.* [13] discussed the threshold function influence in the VMD method, the scaling exponent obtained by detrended fluctuation analysis (DFA) is used as a threshold to distinguish random noise and signal between IMFs and the reconstruction residual. However, these methods are meant for single channels. The method of extending VMD to complex value signal processing was proposed in 2017 [14]. The filter bank structure of complex VMD was studied, and the bi-directional T-F spectrum of complex data based on complex VMD was proposed. But it only applies to bivariate data that contains two channels.

In 2019, ur Rehman and Aftab [15] first proposed the multivariable variational mode decomposition (MVMD) algorithm, which is the extension of the VMD algorithm for the multivariable or multichannel data set. Reference [15] focuses on the ability of MVMD to produce joint oscillation patterns in multivariate data, which is a prerequisite for many practical applications involving non-stationary multivariate data. But [15] doesn't deal with signal denoising. On this basis, this paper proposes a novel multivariate variational mode decomposition denoising scheme that computed the Hausdorff distance (HD) and combined with the subspace (MVMD-HDSP). The proposed algorithm decomposes the multivariable data by MVMD, and then estimates the PDF of each extracted joint rotation mode. Next, based on the similarity measure between the PDF of the input signal and the PDF of each mode, the interval threshold and partial reconstruction are applied to denoise the BLIMFs through HD. Finally, using the characteristics of channel diversity, the subspace projection method is employed to further denoise the multivariable signals. In the process of denoising, this method can not only fuse the internal correlation between multiple

data channels but also can yield joint oscillatory modes in multivariate data which is very effective to denoise non-stationary multivariate data. To verify the effectiveness of the proposed scheme, the synthetic signal and the real signal are simulated to support the analysis.

The structure of this paper is as follows. The second section introduces the principle of the algorithm. In the third section, the multivariable denoising method based on MVMD is presented in detail. In the fourth section, the performance of the algorithm is verified by simulation, and the conclusion is drawn in the fifth section.

## II. BRIEF DESCRIPTION OF MULTIVARIATE VARIATIONAL MODE DECOMPOSITION

The first extension of VMD namely multivariate VMD (MVMD) was proposed by Naveed ur Rehman and Hania Aftab in 2019 [15]. The key of MVMD is to extract  $K$  numbers of predefined multivariable modulation oscillations  $u_k(t)$  from the input data  $x(t)$  containing  $N$  data channels, that is,  $x(t) = [x_1(t), x_2(t), \dots, x_N(t)]$

$$x(t) = \sum_{k=1}^K u_k(t), \quad (1)$$

in which  $u_k(t) = [u_1(t), u_2(t), \dots, u_N(t)]$ .

When extracting the multivariable modulation oscillation set  $\{u_k(t)\}_{k=1}^K$  from the input data, firstly, the sum of the bandwidth of the extracted mode should be minimized. Secondly, the extracted modes can accurately recover the original signal. We estimate the bandwidth of  $u_k(t)$  using the  $L_2$  norm of the gradient function of analytic representation  $u_k^+(t)$ . The cost function of MVMD thus becomes the multivariate extension of the cost function used in the corresponding VMD optimization problem and is given by

$$g = \sum_k \left\| \partial_t \left[ e^{-j\omega_k t} u_k^+(t) \right] \right\|_2^2, \quad (2)$$

in Eq.(2), a single frequency component  $\omega_k$  is used for the harmonic mixing of the entire vector  $u_k^+(t)$ . So, in  $u_k(t)$ . We need to look for multivariate oscillations with a single common frequency component  $\omega_k$  in all channels. To estimate the bandwidth of modulated multivariate oscillations, we should shift the unilateral frequency spectrum in all channels of  $u_k^+(t)$  with the central frequency  $\omega_k$  and take the Frobenius norm of the resulting matrix. The Frobenius norm is taken as a direct extension of the L2 norm used in original VMD to the matrices, which appear due to multiple channel signal representation. And that a simple representation of this function  $g$  is given as follows

$$g = \sum_k \sum_n \left\| u_{k,n}^+(t) e^{-j\omega_k t} \right\|_2^2, \quad (3)$$

in which  $u_{k,n}^+(t)$  is the analytic modulated signal with channel number  $n$  and mode number  $k$ . And  $u_{k,n}^+(t)$  is a complex value signal in the single component. We now give the optimization

problem of the MVMD

$$\min_{\{u_{k,n}\}, \{\omega_k\}} \left\{ \sum_k \sum_n \left\| \partial_t \left[ u_{k,n}^+(t) e^{-j\omega_k t} \right] \right\|_2^2 \right\} \\ s.t. X_N(t) = \sum_k u_{k,n}(t), \quad n = 1, 2, \dots, N. \quad (4)$$

It is important to note that throughout the channel, there are multiple linear equality constraints in the model above. Then the corresponding augmented Lagrangian function will become the following model

$$L(\{u_{k,n}\}, \{\omega_k\}, \lambda_n) \\ = \alpha \sum_{k=1}^K \sum_{n=1}^N \left\| \partial_t u_{k,n}^+(t) e^{-j\omega_k t} \right\|_2^2 \\ + \sum_{n=1}^N \left\| x_n(t) - \sum_{k=1}^K u_{k,n}(t) \right\|_2^2 \\ + \sum_{n=1}^N \left\langle \lambda_n(t), x_n(t) - \sum_{k=1}^K u_{k,n}(t) \right\rangle, \quad (5)$$

where,  $\alpha$  is the balancing parameter of the “data-fidelity” constraint. We suggest making use of the Alternate Direction Method of Multipliers (ADMM) [16] to solve the corresponding unconstrained problem in Eq.(5). ADMM turns the whole optimization problem into a series of iterative sub-optimization problems. These sub-problems are easy to deal with because they seek to minimize the cost function by iterating over a single parameter/function of interest, rather than optimizing the cost function for all optimization variables simultaneously. All the estimated modes in the frequency domain can be expressed as

$$\hat{u}_{k,n}^{l+1}(\omega) = \frac{\hat{x}_n(\omega) - \sum_{i=1}^{k-1} \hat{u}_{i,n}^{l+1}(\omega) - \sum_{i=k+1}^K \hat{u}_{i,n}^l(\omega) + \frac{\hat{\lambda}^l(\omega)}{2}}{1 + 2\alpha(\omega - \omega_k^l)^2}, \quad (6)$$

in which  $\hat{x}_n(\omega)$ ,  $\hat{\lambda}(\omega)$ ,  $\hat{u}_{i,n}(\omega)$ , and  $\hat{u}_k^{n+1}(\omega)$  denote Fourier transforms of  $x_n(\omega)$ ,  $\lambda(\omega)$ ,  $u_{i,n}(\omega)$ , and  $u_k^{n+1}(\omega)$ , respectively, and the  $l$  is the iterations. Because wiener filter is embedded in the algorithm, the VMD is more robust to sampling and noise.

The estimated center frequency of the mode can be obtained by the following formula

$$\omega_k^{l+1} = \frac{\int_0^\infty \omega \left| \hat{u}_{k,n}^{l+1}(\omega) \right|^2 d\omega}{\int_0^\infty \left| \hat{u}_{k,n}^{l+1}(\omega) \right|^2 d\omega}, \quad (7)$$

in which the new  $\omega_k$  is calculated at the center of gravity of the associated the power spectrum of modes.

### III. DENOISING APPROACH

For the signal polluted by Gaussian noise, the denoising method based on VMD is better than that based on wavelet

and EMD [17]. From [15], we can obtain that MVMD algorithm not only inherits all the advantages of VMD algorithm, MVMD also provides dyadic binary filter bank performance for WGN. In this section, Hausdorff distance is used to calculate the distance measure of pdfs, and VMD denoising based on [12] is extended to multivariate signals. The WGN component is then separated from the selected BLIMFs using an interval threshold.

#### A. PROBLEM FORMULATION

Consider a noiseless signal  $y(t)$  transmitted over multiple channels, which is received by multiple sensors, with varying attenuation and time delays contaminated by the white Gaussian noise  $n_i(t)$

$$s_i(t) = b_i y(t - \tau_i) + n_i(t), \quad i = 1, 2, \dots, N, \quad (8)$$

in which  $b_i$  is the propagation attenuation and  $\tau_i$  represents the delay of signals from the  $i_{th}$  sensor,  $N$  denotes the number of channels.

When the MVMD method is used to decompose the signal  $s_i(t)$  from low-frequency to high-frequency, the noiseless signal mode is mainly the low frequency mode, while the noise signal mode is mainly the high frequency mode. The decomposition process as follows

$$s(t) = \sum_{m=1}^M BLIMF_m + \sum_{m=M+1}^K BLIMF_m + r(t), \quad (9)$$

in which  $K$  represents the number of all decomposition modes and  $r(t)$  represents the residue. BLIMF stands for band-limited intrinsic mode functions. In Eq.(9), the modal function from  $BLIMF_1$  to  $BLIMF_M$  are the noiseless signal modes, while the other modes are the noise modes. The purpose of the decomposition is to get an estimate  $\hat{y}(t)$  of the variable  $y(t)$  from  $s(t)$

$$\hat{y}(t) = \sum_{m=1}^{m=M_1} BLIMF_m + \sum_{m=M_1+1}^{m=M} BLIM\hat{F}_m \\ 1 < M_1 < M < K, \quad (10)$$

in which  $BLIM\hat{F}_m$  is the thresholded modes,  $M_1$  and  $M$  denotes the BLIMF indexes for the local reconstruction. In the case of WGN, it is beneficial to remove the noise in high-order BLIMFs and carry out optional thresholding for low-order BLIMFs with low noise energy.

#### B. IDENTIFICATION OF RELEVANT MODES FOR PARTIAL RECONSTRUCTION

In linear signal decomposition and time-frequency decomposition, predefined basis functions are obtained by selecting orthogonal structures. This ensures that there is no “leakage” of information between different modes and channels. It has been proved in [15] that MVMD can be decomposed into almost orthogonal rotation modes. With the increase of the BLIMF order, the frequency content of joint rotational modes changes from slow to fast. When MVMD algorithm

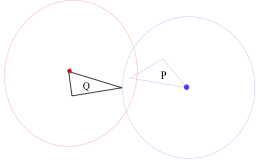


**FIGURE 1.** Hausdorff distance  $H(P, Q)$  for the triangles (the radius of each circle is Hausdorff distance).

is applied to the noise data, the explanation of the extracted rotation mode is necessary to determine which mode contains noiseless signal, which one contains noise signal, or which one contains both.

PDF can reflect the difference between the signal distribution. For this reason, we can obtain the pdfs of the input signal and each mode by kernel density estimation. By calculating the similarity between the pdfs, we can distinguish the relevant mode and the irrelevant mode. Hausdorff distance (HD) is a nonlinear operator used to measure the similarity between two sets or two geometric shapes. With the distance to the corresponding sets increases, the contribution of sets becomes more and more critical in the HD, so HD can be used to determine the geometric distance between densities. The radius of each circle in Fig. 1 is Hausdorff distance  $H(P, Q)$  and Fig. 1 shows that Hausdorff distance gives an interesting measure of their mutual proximity, by indicating the maximal distance between any point of one polygon to the other polygon. Better than the shortest distance, which applied only to one point of each polygon, irrespective of all other points of the polygons. For multi-channel, the two pdfs represented by  $P$  and  $Q$ , the Hausdorff distance is defined as follows

$$HD(P, Q) = \max(D(P, Q), D(Q, P)), \quad (11)$$

$$D(P, Q) = \sum_{i=1}^N \sum_{j=1}^M \max_{p_{ij} \in P} \min_{q_{ij} \in Q} \|p_{ij} - q_{ij}\|, \quad (12)$$

$$D(Q, P) = \sum_{j=1}^M \sum_{i=1}^N \max_{q_{ij} \in Q} \min_{p_{ij} \in P} \|q_{ij} - p_{ij}\|, \quad (13)$$

in which  $N$  denotes the number of channels, and  $M$  is the number of the samples. In order to get the relevant modal function, the similarity operator  $D(\cdot)$  is used to calculate the distance between the  $m$ -dimensional signal  $s(t)$  and the  $n_{th}$  BLIMF component.

$$L(n) = \frac{D}{1 \leq n \leq N} [f(s(t)), f(BLIMF_n(t))], \quad (14)$$

where  $D(\cdot)$  is the HD operator in Eq. (11), and  $f(\cdot)$  is a function of the pdf of the signal. When the distance  $L$  reaches the local maximum for the first time, a subsequent mode is taken as the last BLIMF component of the partial reconstruction.

By calculating the slope of the distance between adjacent BLIMFs, the corresponding mode can be identified. If the slope increases significantly, the similarity occurring after the BLIMF will decrease rapidly. We define  $\alpha$  as the maximum slope of the distance between two adjacent modes and the

input signal.

$$\alpha = \max |L(n) - L(n+1)|, \quad n = 1, 2, \dots, N-1. \quad (15)$$

The index of this  $k_{th}$  mode is identified by  $k_{th} = n$ .

### C. DENOISING BASED ON INTERVAL THRESHOLD

Although partial reconstruction can effectively suppress the out-of-band noise, the noise in the same BLIMF component as the signal cannot be effectively eliminated. Because MVMD has good dyadic filter bank characteristics for WGN [15], and it is generally believed that the last BLIMF component contains most of the noise, so the noise power  $E_n$  in the  $n_{th}$  BLIMF decomposed by MVMD can be approximated by the power  $E_N$  of the last BLIMF decomposed by MVMD.

$$E_n = \frac{E_N}{\beta} \rho^{-n}, \quad n = 1, 2, \dots, N-1, \quad (16)$$

in which both  $\beta$  and  $\rho$  are parameters could be obtained from a large number of experimental statistical results. According to wavelet threshold denoising method, a universal threshold is

$$T_n = C \sqrt{E_n 2 \ln M}, \quad (17)$$

in which  $T_n$  is the threshold value of the  $n_{th}$  BLIMF decomposed by MVMD,  $M$  represents the length of data and  $C$  denotes a constant that increases the flexibility of the threshold.

The direct application of either hard threshold or soft threshold will lead to the discontinuity of reconstructed signals. Because BLIMF is an amplitude-modulated-frequency-modulated (AM-FM) signal with a mean of zero. Therefore, whether it is related to noise or not, it makes no sense for any isolated BLIMF sample. The interval threshold is to take the signal  $W_n^m = [w_n^m, w_{n+1}^m]$  between two adjacent zero intersection as a whole to judge whether it is noise dominant or signal dominant according to the unipolar value  $h_m(r_n^m)$  related to this interval. Therefore, the soft interval threshold is converted to

$$\hat{h}_m(W_n^m) = \begin{cases} 0, & |h_m(r_n^m)| \leq T_n \\ \text{sgn}(h_m(W_n^m))(|h_m(W_n^m)| - T_n), & \text{else.} \end{cases} \quad (18)$$

Different from the method of local reconstruction or thresholding used in the univariate VMD denoising method, both methods are introduced in this paper to the MVMD denoising method, hereinafter referred to as MVMD-HD. The calculated  $k_{th}$  is the best candidate for  $M$  only for a single local reconstruction [10]. But some high-frequency components with smaller amplitudes will be removed. An empirical way to choose the corresponding modes could be

$$M = \max(1, k_{th} - P), \quad (19)$$

in which  $P$  denotes a constant that can be obtained after many experiments according to the signal characteristics. Generally, the appropriate value of  $P$  is considered to be  $P = 4$ , and as a rule of thumb,  $M1$  is considered to be 1, which is the result of repeated simulations of multiple data sets.



#### D. DENOISING COMBINED WITH SUBSPACE PROJECTION

In the MVMD-HD method proposed in the previous section, BLIMFs is partially reconstructed using the mode alignment characteristics of MVMD. However, the interval threshold is channel-wise and does not consider the correlation within the same index BLIMFs. Therefore, on the basis of the proposed denoising scheme (MVMD-HD), we further make full use of the subspace projection scheme to exploit the inter-channel correlation in the input data.

If the receiving signal  $s_i(t)$  from multiple sensors are considered to be synchronous, that is, the  $\tau_i$  in Eq.(8) is equal to 0, the signals received in Eq.(8) can be represented as the following matrix

$$S = BY + G = [s_1, s_2, \dots, s_N] \in C^{M \times N}, \quad (20)$$

in which  $M$  and  $N$  represent the number of observed sample points and channels, respectively.  $G$  is a Gaussian noise of unknown covariance matrix  $\Sigma_g$ . The covariance matrix of the observation signal matrix  $S$  is

$$R_S = E(S^T S). \quad (21)$$

As the signal of interest in different channels are highly correlated, the covariance matrix  $R_S$  can be further decomposed by singular value decomposition (SVD) as

$$\begin{aligned} R_S &= U \Sigma U^T = [U_z, U_n] \begin{bmatrix} \Sigma_z O \\ O \Sigma_n \end{bmatrix} \begin{bmatrix} U_z^T \\ U_n^T \end{bmatrix} \\ &= U_z \Sigma_z U_z^T + U_n \Sigma_n U_n^T, \end{aligned} \quad (22)$$

where,

$$\begin{aligned} U_z &\stackrel{\text{def}}{=} [u_1, u_2, \dots, u_r] \\ U_n &\stackrel{\text{def}}{=} [u_{r+1}, u_{r+2}, \dots, u_N] \\ \Sigma_z &= \text{diag}(\sigma_{z1}^2 + \sigma_{g1}^2, \sigma_{z2}^2 + \sigma_{g2}^2, \dots, \sigma_{zr}^2 + \sigma_{gr}^2) \\ \Sigma_n &= \text{diag}(\sigma_{gr+1}^2, \sigma_{gr+2}^2, \dots, \sigma_{gN}^2), \end{aligned} \quad (23)$$

where  $\sigma_i^2$  and  $\gamma_i^2$  represent the nonzero eigenvalues of signal and noise in the  $i$ th column, respectively. Thus, the observation matrix  $S$  can be projected into the signal subspace,  $\text{Span}(U_z) = \text{Span}\{u_1, u_2, \dots, u_r\}$  and noise subspace,  $\text{Span}(U_n) = \text{Span}\{u_{r+1}, u_{r+2}, \dots, u_N\}$  by multiplying the orthogonal matrix  $U$ .

$$F = SU. \quad (24)$$

The subspace projection makes full use of the spatial diversity characteristics of the observed signal  $S$ , and the signal energy produces a focusing effect in the pre- $r$ -dimensional space, which improves the signal to noise ratio in the signal subspace, and the transformed signal to noise ratio can be expressed as

$$\begin{aligned} \text{SNR} &= 10\log_{10} \left( \frac{P_z}{r/NP_g} \right) \\ &= 10\log_{10} \left( \frac{N}{r} \right) + 10\log_{10} \left( \frac{P_z}{P_g} \right), \end{aligned} \quad (25)$$

in which,  $P_z$  and  $P_g$  denote the signal power and the noise power respectively. It can be seen that the signal in the front  $r$  dimension will obtain a total  $10\log_{10} \left( \frac{N}{r} \right)$  gain of SNR by changing the bases.

Because MVMD can be regarded as a linear decomposition, the gain of subspace projection will be obtained through the transformation of BLIMFs. The received signal will be decomposed into

$$C = \Re S = [C_1, C_2, \dots, C_K], \quad (26)$$

in which  $\Re$  represents the MVMD operator,  $C$  contains the joint rotational modes and  $C_i$  is the  $i$ th BLIMF component selected for thresholding, the subspace projection of  $C_i$  can obtain a certain SNR gain, and the corresponding orthogonal transform for  $C_i$  is

$$\tilde{C}_i = U^T C_i, \quad (27)$$

According to Eq.(10), the first  $M1$  BLIMFs components are unprocessed, and the last  $K - M + 1$  BLIMFs directly discarded. So in order to reduce complexity, only the components that need to be thresholded can be performed subspace transformation, and the thresholded BLIMFs after inverse transform can be written as

$$\hat{C}_i = U \tilde{C}_i, \quad (28)$$

in which  $\hat{C}_i$  denotes the BLIMFs processed by thresholded in the transformation domain. Consequently, the finally denoising matrix  $\hat{F}$  can be well recovered well by the following formula

$$\hat{F} = \Re^{-1} \hat{C}, \quad (29)$$

in which  $\hat{C}$  includes the BLIMF subset  $\{\hat{C}_i\}$  processed by thresholded and the unprocessed subset  $\{C_j\}$ . Next, we will call this denoising method MVMD-HDSP.

#### IV. SIMULATION RESULTS AND DISCUSSION

In this paper, the performance of the proposed multivariate variational mode decomposition combined with the subspace algorithm will be evaluated by comparing it with the latest technology of multi-component signal denoising: multivariate denoising using wavelet and principal component analysis (MWD) [3], multivariate empirical mode decomposition based interval thresholding (MEMD-IT) and the MEMD-IT in conjunction with subspace projection (MEMD-ITSP) [10]. The synthetic quadrivariate signals with a length of 2048 used in the experiment consisting of 'Blocks', 'Bumps', 'Heavy Sine' and 'Doppler' in its four channels. We also use amplitude modulated and frequency modulated (AM-FM) synthetic signal Eq.(30) [12] with a length of 2048 to form multi-channel signals.

$$\begin{aligned} s &= (1 + 0.5 * \cos(2 * \pi * 24 * t)) \\ &\quad * \cos(2 * \pi * 40 * t + \cos(2 * \pi * 5 * t)). \end{aligned} \quad (30)$$

In addition, real world multivariate data sets are test in our experiments, a trivariate wind speed signal with the length

of 1440 obtained from a site in Jhimpir, Pakistan while the bivariate float drift data with the length of 1116 was taken during the Eastern Basin experiment (Sofar data) [18]. Via through repeating simulation of multiple data sets, we take the balancing parameter  $\alpha = 2000$ , while for the heavy sine signal and doppler signal, the mode number parameter  $K = 15$ , and  $K = 5$  in the rest of the test signals.

### A. DENOISING PERFORMANCE OF SYNTHETIC DATA SETS

The proposed method and the comparison method are applied to the synthetic quadrivariate data which were added to the multivariate Gaussian noise samples with balanced input SNR = 5dB which is shown in Fig.2, and the resultant denoised synthetic quadrivariate data are shown in Fig.3(a)-Fig.3(d).

Table1 shows the average reconstructed SNR value of denoising signal, calculated by  $I = 10$  iterations, calculated

**TABLE 1. SNR performance of different methods for synthetic quadrivariate signal.**

Denoising method	Signal types	SNR				
		-4dB	-2dB	0dB	2dB	5dB
MWD	Blocks	10.66	11.82	12.29	12.98	13.17
	Bumps	1.09	0.74	0.83	0.90	1.02
	Heavy sine	12.83	14.08	16.87	17.25	19.07
	Doppler	<b>0.328</b>	<b>0.53</b>	0.19	0.66	0.71
MEMD-IT	Blocks	10.57	11.61	13.18	15.31	16.84
	Bumps	7.14	9.62	12.17	12.49	<b>14.89</b>
	Heavy sine	13.24	16.52	17.05	18.27	21.16
	Doppler	7.18	5.71	-2.82	-2.58	1.76
MEMD-ITSP	Blocks	10.52	11.38	13.29	14.82	16.68
	Bumps	6.79	9.5	11.87	12.21	14.78
	Heavy sine	13.01	16.46	16.61	18.07	19.69
	Doppler	7.31	5.79	-2.66	-2.36	1.32
MVMD-HDSP	Blocks	<b>11.03</b>	<b>13.23</b>	<b>14.14</b>	<b>15.92</b>	<b>16.85</b>
	Bumps	<b>7.61</b>	<b>9.72</b>	<b>12.18</b>	<b>12.82</b>	14.16
	Heavy sine	<b>16.58</b>	<b>17.92</b>	<b>20.51</b>	<b>22.23</b>	<b>23.53</b>
	Doppler	3.94	2.56	<b>0.2</b>	<b>3.10</b>	<b>5.00</b>

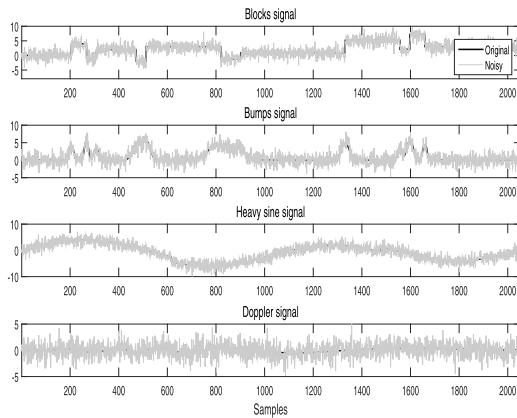


**FIGURE 2. Time plots of synthetic quadrivariate signal (black) along with its noisy versions (gray).**

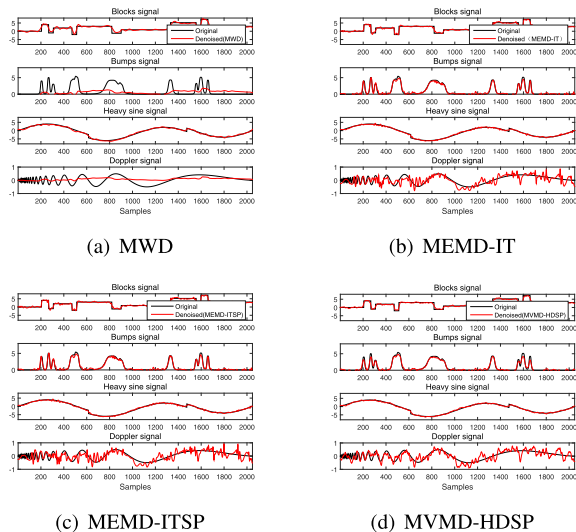


**FIGURE 3. Time plots of synthetic quadrivariate signal along with the its denoised versions obtained from MWD (top left), MEMD-IT (top right), MEMD-ITSP (bottom left) and the proposed MVMD-HDSP (bottom right).**

by MWD, MEMD-IT and MEMD-ITSP, and the proposed MVMD-HDSP algorithm for the input SNR range of balanced noise ( $-4\text{dB}$  to  $5\text{dB}$ ). and the best results are in bold.

As can be seen from the Fig.3 and Table 1, MWD's performance is generally poor, although it produces a relatively high reconstructed SNR at a lower noise level (a higher input SNR), it consistently performs poorly at a higher noise level (a lower input SNR). MEMD-IT performs poorly in most cases because they perform channel-by-channel de-noising, ignoring inter-channel correlation in the data. Under a large range of input SNR, due to the nature of Hausdorff distance and the subspace operation characteristics of the proposed MVMD, this method has a stronger ability to fuse inter-channel correlation than MEMD-ITSP, therefore MVMD-HDSP method is always superior to all other comparison methods.

In order to evaluate the denoising effect of MVMD-HDSP, we used amplitude modulated and frequency modulated (AM-FM) signal with SNR between  $-4\text{dB}$  to  $4\text{dB}$  to form multi-channel signals for testing, it is representative of non-linear and non-stationary signal. The AM-FM signal Eq.(30) is shown in Fig.4.

### 1) INFLUENCE OF ASYNCHRONOUS FACTORS

Due to the influence of signal transmission environment, most of the different channels have asynchronous characteristics, so it is of great significance to study the asynchronous characteristics among signal channels. To analyze the performance of different methods on signals with asynchronous characteristics, we used amplitude modulated and frequency modulated (AM-FM) signal to form multi-channel signals for testing, taking into account different time offsets.

The joint denoising effect of different algorithms on asynchronous signals is shown in Fig.5. In order to avoid complexity, two signal channels are used in the simulation experiment, and the input SNR in different channels is  $2\text{dB}$ . When the number of offset points  $\Delta \leq 40$  (approximately 2% of the

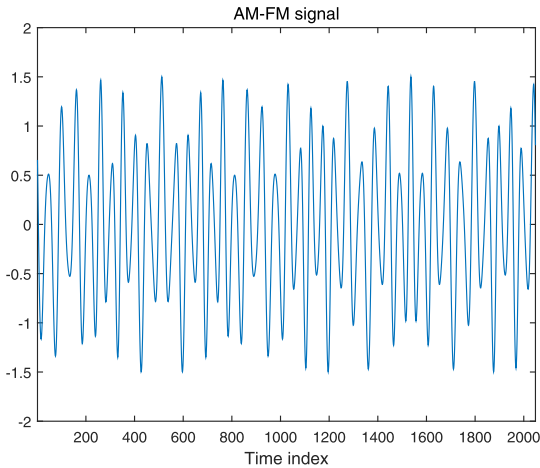


**FIGURE 4.** Amplitude modulated and frequency modulated (AM-FM) signal.

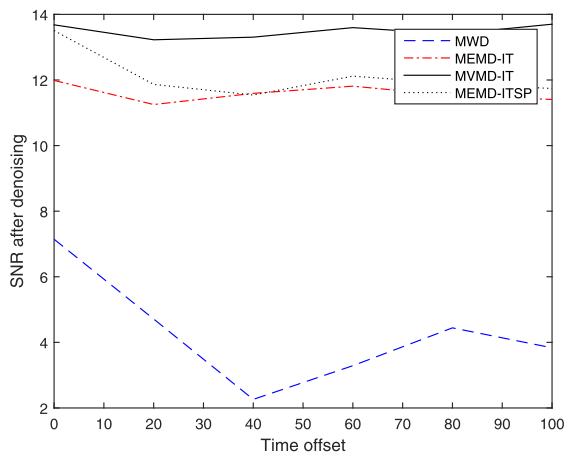


**FIGURE 5.** Performance comparison of different algorithms for interference suppression under asynchronous condition.

signal length), the performance of MWD based algorithms degrades significantly, and the performance of MWD algorithm is also very poor when the number of offset points  $n > 40$ . The orthogonal transformation and principal component analysis methods used in MWD are linear and not fit for the asynchronous signals. The MEMD-IT algorithm is insensitive to time offset because it does not perform the linear transformation of signals between different channels. At the same time, the MEMD-ITSP method depends on the time offset between channels. Therefore, the denoising performance of the MEMD-ITSP algorithm decreases with the increase of time offset. In contrast, the MVMD-HDSP achieves an almost constant improvement of SNR relative to the time offset, and its performance is the best, for it can fuse the internal correlation between multiple data channels.

## 2) INFLUENCE OF CHANNEL NOISE UNBALANCED POWER FACTOR

We also consider the simulation of unbalanced power in the data channel, for simplicity, let's just consider the synchronization case in the four channels. The SNR of the

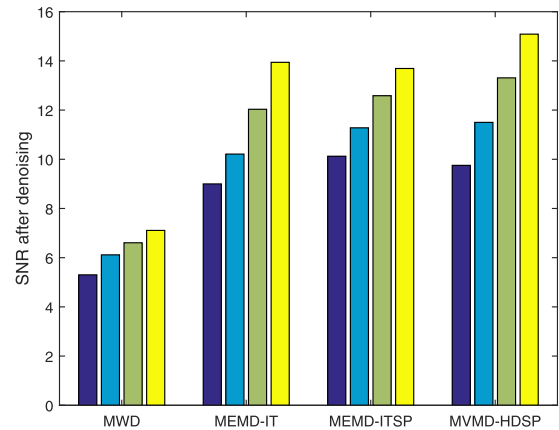


**FIGURE 6.** Performance comparison of different algorithms for interference suppression under unbalanced power condition.

four channels are  $-2\text{dB}$ ,  $0\text{dB}$ ,  $2\text{dB}$  and  $4\text{dB}$  respectively. Fig.6 shows the results of the ensemble average of 10 independent noises. The PCA method in the MWD algorithm is a linear transformation, which leads to the pollution of the signal in the high SNR channel by the low SNR signal, resulting in the poor denoising performance of the MWD algorithm. Due to the application of subspace projection, MEMD-ITSP and MVMD-HDSP can make use of the correlation between channels and better than MEMD-IT approach regardless of the signal form. In addition, owing to the mode-alignment property of MVMD-HDSP, its denoising effect is better than that of MEMD-ITSP.

## B. DENOISING PERFORMANCE OF REAL WORLD DATA

In addition to the synthetic signals, we have included denoising results on the real world multivariate data sets of a trivariate wind speed signal (with speeds along east-west, north-south and vertical directions in its three channels) and a sofar bivariate signal. The wind data were recorded from a wind power generating site in Jhimpir, Pakistan while the bivariate float drift data was taken during the Eastern Basin experiment. Fig.7 and Fig.9 respectively show the trivariate wind speed signal (black) and its noisy version (gray), sofar bivariate signal (black), and its noisy version (gray). Both of these noisy versions were added in the multivariable WGN sample with balanced input SNR of  $4\text{dB}$ . The resultant denoised trivariate and bivariate real world data from MWD, MEMD-IT, MEMD-ITSP and the proposed MVMD-HDSP are respectively shown in Fig.8(a)-Fig.8(d) and Fig.10 (a) to Fig.10 (d). In addition, their corresponding SNR is shown in Table 2 and Table 3, respectively.

All of these methods have sound effects, but the method proposed in this paper has an excellent tracking effect on the original signal, especially in the period when the input signal changes much, such as the time index = 600 and the endpoint (time index = 1400) of the trivariate wind speed signal.

Indeed, in Table 2 and Table 3, the quantitative results of extensive experiments performed on real signals have been provided. The average reconstruction SNR of the denoised

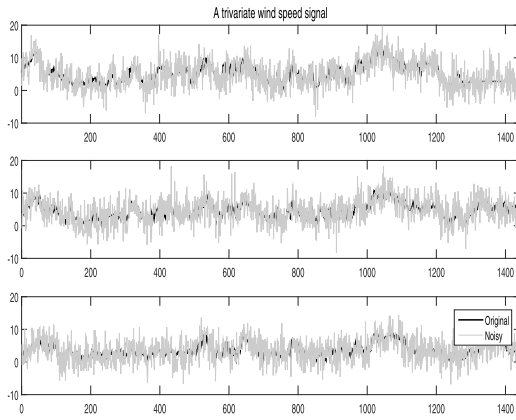


**FIGURE 7.** Time plots of trivariate real world signal (black) along with the noisy versions (gray).

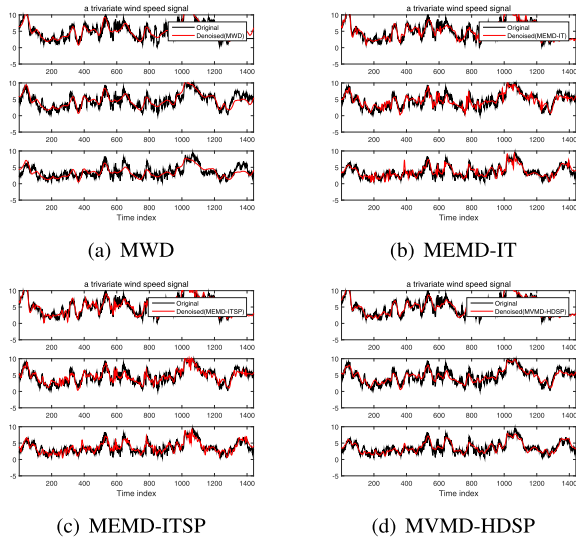


**FIGURE 8.** Time plots of trivariate real world signal along with its denoised versions obtained from MWD (top left), MEMD-IT (top right), MEMD-ITSP (bottom left) and the proposed MVMD-HDSP (bottom right).

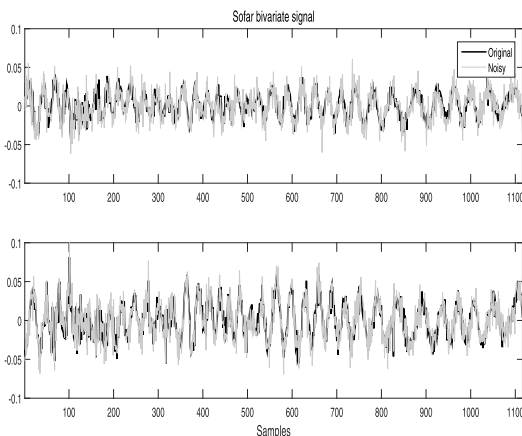


**FIGURE 9.** Time plots of bivariate real world signal (black) along with the noisy versions (gray).

signal is shown in Table 2 and Table 3, calculated by  $I = 10$  iterations, calculated by MWD, MEMD-IT and MEMD-ITSP, and the proposed MVMD-HDSP algorithm for the

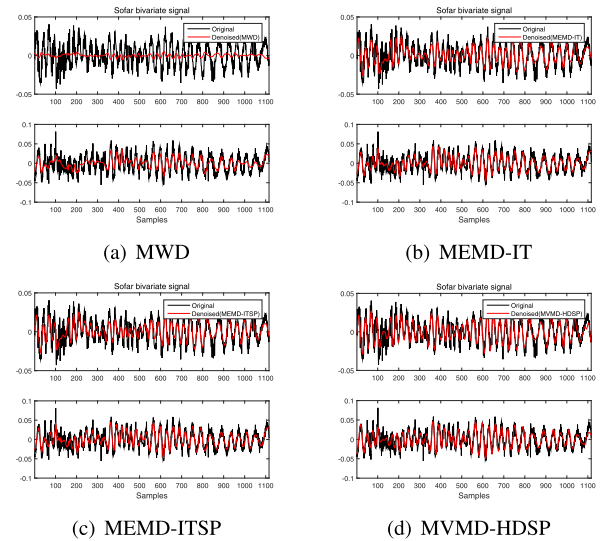


**FIGURE 10.** Time plots of bivariate real world signal along with its denoised versions obtained from MWD (top left), MEMD-IT (top right), MEMD-ITSP (bottom left) and the proposed MVMD-HDSP (bottom right).

**TABLE 2.** SNR performance of different methods for trivariate real world signal.

Denoising method	Channel	SNR				
		-4dB	-2dB	0dB	2dB	4dB
MWD	First channel	10.45	11.50	12.23	12.12	13.37
	Second channel	10.30	10.70	12.67	13.12	13.08
	Third channel	<b>9.55</b>	<b>10.41</b>	10.91	11.35	10.90
MEMD-IT	First channel	11.21	11.55	12.75	13.90	15.20
	Second channel	9.37	10.68	11.23	12.88	13.97
	Third channel	7.48	9.17	10.74	11.72	13.15
MEMD-ITSP	First channel	10.98	11.52	12.95	13.72	15.49
	Second channel	9.21	11.17	11.85	13.81	14.46
	Third channel	7.36	9.32	10.81	12.00	13.25
MVMD-HDSP	First channel	<b>11.25</b>	<b>11.66</b>	<b>13.58</b>	<b>14.58</b>	<b>15.53</b>
	Second channel	<b>10.31</b>	<b>11.45</b>	<b>12.71</b>	<b>13.88</b>	<b>14.47</b>
	Third channel	8.40	9.40	<b>11.51</b>	<b>12.57</b>	<b>13.97</b>

**TABLE 3.** SNR performance of different methods for bivariate real world signal.

Denoising method	Channel	SNR				
		-4dB	-2dB	0dB	2dB	4dB
MWD	First channel	-0.01	0.06	0.03	0.04	0.04
	Second channel	0.76	1.05	2.10	2.78	3.34
MEMD-IT	First channel	3.13	3.62	4.41	5.40	5.45
	Second channel	3.65	4.32	5.60	5.90	6.07
MEMD-ITSP	First channel	3.09	3.57	4.61	4.92	5.28
	Second channel	3.79	4.31	5.71	5.82	6.18
MVMD-HDSP	First channel	<b>3.61</b>	<b>4.39</b>	<b>5.08</b>	<b>5.85</b>	<b>6.02</b>
	Second channel	<b>4.72</b>	<b>5.16</b>	<b>6.17</b>	<b>5.99</b>	<b>6.20</b>

input SNR range of balanced noise ( $-4$ dB to  $4$ dB), and the best results are in bold.

Because the trivariate wind speed signal and the sofars bivariate signal have the short stationary characteristics, and the frequency change is slow, the four methods achieve good denoising effect. However, under the condition of low SNR, the MWD algorithm has high reconstruction SNR values because of its own characteristics. From the whole range of SNR ( $-4$ dB to  $4$ dB), the MVMD-HDSP method



outperformed, and the SNR of this method is improved by 1dB to 2dB compared with other methods, which verifies the effectiveness of the algorithm.

## V. CONCLUSION

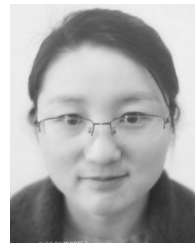
A novel multivariate variational mode decomposition based denoising method using subspace projection (MVMD-HDSP) is proposed in this paper. This method attempts to eliminate the noise in the input data by the statistical difference between the pdfs of WGN and the expected data. We used Hausdorff distance to calculate the pdf distance of multivariate matrices, and interval threshold for the identified BLIMFs. Both the synthetic and real world multivariate data are tested using four different algorithms. Simulation results show that the MVMD-HDSP algorithm has a better denoising effect than based on the MEMD algorithm and wavelet methods. This is because MVMD is more robust to WGN in that the mode-alignment of the MVMD algorithm is more obvious than that of the MEMD algorithm, resulting in well-defined subband filters than the MEMD algorithm.

## ACKNOWLEDGMENT

The authors thank Prof. N. U. Rehman for providing them the code of his method.

## REFERENCES

- [1] P. C. Ching, H. C. So, and S. Q. Wu, "On wavelet denoising and its applications to time delay estimation," *IEEE Trans. Signal Process.*, vol. 47, no. 10, pp. 2879–2882, Oct. 1999.
- [2] C. Park, D. Looney, N. U. Rehman, A. Ahrabian, and D. P. Mandic, "Classification of motor imagery BCI using multivariate empirical mode decomposition," *IEEE Trans. Neural Syst. Rehabil. Eng.*, vol. 21, no. 1, pp. 10–22, Jan. 2013.
- [3] M. Aminghafari, N. Cheze, and J.-M. Poggi, "Multivariate denoising using wavelets and principal component analysis," *Comput. Statist. Data Anal.*, vol. 50, no. 9, pp. 2381–2398, May 2006.
- [4] R. Yang and M. Ren, "Wavelet denoising using principal component analysis," *Expert Syst. Appl.*, vol. 38, no. 6, p. 7910, 2011.
- [5] A. Ahrabian and D. Mandic, "A class of multivariate denoising algorithms based on synchrosqueezing," *IEEE Trans. Signal Process.*, vol. 63, no. 9, pp. 2196–2208, May 2015.
- [6] D. P. Mandic, N. U. Rehman, Z. Wu, and N. E. Huang, "Empirical mode decomposition-based time-frequency analysis of multivariate signals: The power of adaptive data analysis," *IEEE Signal Process. Mag.*, vol. 30, no. 6, pp. 74–86, Nov. 2013.
- [7] H. Hao, H. Wang, W. Zeng, and H. Tian, "MEMD-based filtering using interval thresholding and similarity measure between pdf of IMFs," *IEICE Trans. Fundam. Electron., Commun. Comput. Sci.*, vol. E99.A, no. 2, pp. 643–646, 2016.
- [8] D. Looney, V. Goverdovsky, P. Kidmose, and D. P. Mandic, "Subspace denoising of EEG artefacts via multivariate EMD," in *Proc. IEEE Int. Conf. Acoust., Speech Signal Process. (ICASSP)*, May 2014, pp. 4688–4692.
- [9] N. U. Rehman and D. P. Mandic, "Filter bank property of multivariate empirical mode decomposition," *IEEE Trans. Signal Process.*, vol. 59, no. 5, pp. 2421–2426, May 2011.
- [10] H. Hao, H. L. Wang, and N. U. Rehman, "A joint framework for multivariate signal denoising using multivariate empirical mode decomposition," *Signal Process.*, vol. 135, pp. 263–273, Jun. 2017.
- [11] K. Dragomiretskiy and D. Zosso, "Variational mode decomposition," *IEEE Trans. Signal Process.*, vol. 62, no. 3, pp. 531–544, Feb. 2014.
- [12] W. Ma, S. Yin, C. Jiang, and Y. Zhang, "Variational mode decomposition denoising combined with the hausdorff distance," *Rev. Sci. Instrum.*, vol. 88, no. 3, Mar. 2017, Art. no. 035109.
- [13] F. Li, B. Zhang, S. Verma, and K. J. Marfurt, "Seismic signal denoising using thresholded variational mode decomposition," *Explor. Geophys.*, vol. 49, no. 4, pp. 450–461, Aug. 2018.
- [14] Y. Wang, F. Liu, Z. Jiang, S. He, and Q. Mo, "Complex variational mode decomposition for signal processing applications," *Mech. Syst. Signal Process.*, vol. 86, pp. 75–85, Mar. 2017.
- [15] N. U. Rehman and H. Aftab, "Multivariate variational mode decomposition," *IEEE Trans. Signal Process.*, vol. 67, no. 23, pp. 6039–6052, Dec. 2019.
- [16] M. R. Hestenes, "Multiplier and gradient methods," *J. Optim. Theory Appl.*, vol. 4, no. 5, pp. 303–320, Nov. 1969.
- [17] Y. Liu, G. Yang, M. Li, and H. Yin, "Variational mode decomposition denoising combined the detrended fluctuation analysis," *Signal Process.*, vol. 125, pp. 349–364, Aug. 2016.
- [18] N. U. Rehman, B. Khan, and K. Naveed, "Data-driven multivariate signal denoising using Mahalanobis distance," *IEEE Signal Process. Lett.*, vol. 26, no. 9, pp. 1408–1412, Sep. 2019.



**PEIPEI CAO** received the M.S. degree in communication engineering from Shanghai Maritime University, Shanghai, China, in 2011. She is currently pursuing the Ph.D. degree with the Nanjing University of Science and Technology. Her research interest includes weak signal detection and processing.



**HUALI WANG** (Member, IEEE) received the M.S. and Ph.D. degrees in electronic engineering from the Nanjing University of Science and Technology, China, in 1993 and 1997, respectively. He is currently a Professor with the College of Communication Engineering, PLA Army Engineering University, Nanjing, China. His research interests include wireless and satellite communications, statistical signal, and array processing.



**KAIJIE ZHOU** received the B.S. degree in electrical engineering and automation from the Hefei University of Technology, Hefei, China, in 2007, and the M.S. degree in electrical theory and new technology from Shandong University. He is currently pursuing the Ph.D. degree in signal and information processing with PLA Army Engineering University, Nanjing, China. His research interests include wireless communications and physical-layer security.

...